Sedimentary exhalative venting of bioavailable nitrogen into the early ocean

Eva E. Stüeken[1,*], Daniel D. Gregory[2], Indrani Mukherjee[3], Peter McGoldrick[3]

1. School of Earth & Environmental Sciences, University of St Andrews, North Street, Irvine Building, St Andrews, Fife, KY16 9AL, Scotland, UK
2. Department of Earth Sciences, Earth Sciences Centre, 22 Russell Street, Toronto, Ontario M5S 3B1, Canada
3. CODES & IMAS, University University of Tasmania, Hobart, Tasmania 7001, Australia
* corresponding author (email: ees4@st-andrews.ac.uk)

Abstract

Ore deposits found in Proterozoic marine sedimentary basins supply much of the world's zinc. Many of the deposits formed contemporaneously with their host sediments when saline brines circulating from deeper in the basin reached the sea floor. Textural, geochemical and isotopic features of these SEDEX ('sedimentary-exhalative') deposits and their host sediments indicate that biologically active seeps, vents and brine pools were a feature of many ore-forming systems. In mineralised pockets of mid-Proterozoic basins, these 'microbial oases' were productive areas in an otherwise low productivity, anoxic, deep marine realm. Here we hypothesize that these metal-rich brines which circulated through organic matter-rich substrate also carried high levels of fixed nitrogen and stimulated distinct ecosystems at sites of mineralisation, or enhanced productivity more broadly in the basin. We tested this hypothesis with organic carbon and nitrogen analyses of samples of carbonaceous siltstone and shale from the 1.64 Ga Barney Creek Formation of northern Australia. The Barney Creek Formation hosts several SEDEX Zn systems, including one of the world's largest deposits at McArthur River Mine (the HYC deposit). Samples come from the mineralised edge of HYC and from correlated strata in drill cores at varying distances (1-60 km) from the deposit. The data reveal lower ratios of total organic carbon (TOC) to total nitrogen (TN) closer to the ore body. Strong correlations ($r^2 > 0.7$) between TOC and TN and the absence of excess N in the samples suggest that most N was buried as bound to organic matter. Bioavailable N was thus probably more abundant closer to HYC, consistent with fixed nitrogen input by hydrothermal fluids. If correct, our data may suggest that such a hydrothermal nitrogen point source enabled microbes to develop lower C:N ratios in their biomass. A hydrothermal nitrogen source is also supported by a gradient in $\delta^{15}N$ values from = +4‰ proximal to the vent to +7.5‰ in distal sites, which may point towards recycling of ammonium from the underlying Wollogorang Formation (1.73 Ga). This unit has previously been identified as a source of over-mature hydrocarbons to the ore-forming fluid. We speculate that, during the mid-Proterozoic, fixed nitrogen carried by SEDEX hydrothermal brines may have locally offset the lack of aerobic nutrient remineralization that characterized most of the anoxic Precambrian deep ocean and thus stimulated biological productivity in areas where the brines reached the sea floor, and, possibly, more broadly as spent brines mixed into the water column.

1. Introduction

Recent data suggest that throughout most of the Proterozoic biological productivity was much lower than today (Crockford *et al.*, 2018), possibly due to scarcity of several essential nutrients, including phosphorus and ammonium (Koehler *et al.*, 2017; Reinhard *et al.*, 2017). It has even been proposed, though not proven, that organisms may have had to adjust their biochemical makeup with modified *Redfield* ratios, *i.e.* higher ratios of carbon to nitrogen and phosphorus in their biomass (Planavsky, 2014). Nevertheless, several evolutionary milestones fall into the mid-Proterozoic eon, such as the origin of eukaryotes, crown group diversification, and the invention of sexual reproduction (Knoll & Nowak, 2017). In fact, it is conceivable that some biological innovations were triggered by nutrient scarcity, because these conditions favoured the expansion of "creative" strategies (Mukherjee *et al.*, 2018). It is also possible that localised environmental niches with unusually high nutrient supplies created hotspots of biological productivity, perhaps leading to crowding and more rapid gene exchange. Here we hypothesize that one potentially important type of setting for high rates of biological turnover may have been hydrothermally active basins. Hydrothermal vents in the modern ocean have been shown to disperse essential micronutrients over many kilometres and fuel microbial activity (Ardyna *et al.*, 2019; Schine *et al.*, 2021). It is also known that modern vent fluids are enriched in ammonium (NH_4^+), if they circulate through sedimentary packages (Lilley *et al.*, 1993). Vents thus effectively recycle fixed nitrogen back into the water column. In today's oxic ocean, the major nutrients are recycled by remineralization of organic matter, but this aerobic recycling mechanism would have been suppressed in the Precambrian when the deep ocean was anoxic (Kipp & Stüeken, 2017). We therefore hypothesize that hydrothermal fluids may have locally offset the lack of aerobic biomass remineralization by remobilizing nutrients from buried sedimentary packages. Similar to aerobic recycling within the water column, such processes may have effectively extended the residence time of nutrients in surface environments and created nutrient-rich "oases" for early life.

To test this hypothesis, we investigated samples from the 1.64 Ga Barney Creek Formation of the southern McArthur Basin in northern Australia (Fig. 1). At McArthur River Mine the HYC ('Here's Your Chance') orebody, one of the world's largest sedimentary zinc deposits, is hosted in carbonaceous and pyritic siltstones and shales of the Barney Creek Formation (Section 2). We selected samples from a mine drill core, and from five regional drill cores at varying distances from the mine. The total range in our sample set extends from the edges of the HYC deposit to 55 km away (Fig. 2). We measured nitrogen and organic carbon isotopes and abundances in these samples to test if the hydrothermal fluids that created the HYC mineral deposit also affected the nitrogen cycle. Our results are compatible with the idea that these fluids imported bioavailable nitrogen into the basin that may have fuelled microbial life locally.

2. Geologic Setting

During the late Paleoproterozoic to early Mesoproterozoic, a number of broadly correlative sedimentary basins developed on the attenuated margin of northern Australia (Betts & Giles, 2006). They preserve terrestrial volcano-sedimentary and marine sedimentary sequences ('rift-sag' cycles) deposited between 1.73 Ga and 1.43 Ga (Southgate *et al.*, 2000). In the southern McArthur Basin (Fig. 2), the Tawallah Group (1.76-1.70 Ga) is a rift package up to five kilometres thick comprising terrestrial to shallow marine terrigenous siliciclastics and subaerial volcanics (Pietsch *et al.*, 1991). The Wollogorang Formation (Fig. 1), in the upper Tawallah Group, is a thin (< 100

m), widespread, organic-rich dolomitic shale and dolostone unit that probably formed in slightly deeper water conditions (Donnelly & Jackson, 1988). The Tawallah Group is overlain by the McArthur Group, a tectonic sag package with a composite thickness approaching 4.5 kilometres dominated by platform carbonate facies (bedded and stromatolitic dolomites), local evaporitic facies and tidally-influenced siliciclastics. Tectonically-driven increased accommodation space during mid-Barney Creek times created a series of 'sub-basins' within the carbonate platform (McGoldrick *et al.*, 2010). These preserve deep-water (turbiditic) dolomitic siltstones and carbonaceous and pyritic shales of the Barney Creek Formation (Bull, 1998).

The Barney Creek Formation (Fig. 1) is typically depicted as bracketed by the Teena Dolomite below and the Reward Dolomite above (McGoldrick *et al.*, 2010). However, the thickness of the Barney Creek Formation is highly variable and shale facies are absent in many sections (i.e., the Teena Fm passes directly into Reward Fm). However, in the 'sub-basins' near growth structures (e.g., in the vicinity of HYC) it can develop thicknesses of up to a kilometre. Hence, the Reward-Barney-Teena 'succession' is better considered a partly contemporaneous mosaic of shelf, slope and basinal facies (McGoldrick *et al.*, 2010), deposited on a regionally extensive marine carbonate platform (Kunzmann *et al.*, 2019). Sequence stratigraphic analysis indicates persistent marine conditions during Reward-Barney-Teena times (Southgate *et al.*, 2000), although evaporitic and restricted shallow water facies are present at other stratigraphic levels of the McArthur Group. All known SEDEX Zn mineralisation in the McArthur Basin is confined to the Barney Creek Formation. The thicker shaley facies have been the targets for Zn exploration since the discovery of HYC in the 1950s, and a number of named prospects and 'sub-basins' have been identified. Several prospects and 'sub-basins' are known to occur along the fault structure to the west of HYC (McArthur River area in Fig. 2), and the low-grade Myrtle prospect (~ 2 Mt of contained Zn+Pb) lies just north of the Myrtle sub-basin (Fig. 2). With the notable exception of a new discovery about 12 kilometres west of HYC (the Teena deposit - Taylor *et al.*, 2017), all these prospects contain (at least) an order of magnitude less Zn and Pb than HYC (Teena contains ~ 7 Mt of Zn+Pb compared to ~30 Mt of Zn+Pb at HYC – Taylor *et al.*, 2009; Taylor *et al.*, 2017).

Historically, ideas about the timing of formation of Zn and Pb sulphides in the stratiform Zn-Pb deposits of the Australian Proterozoic Zinc Belt have been contentious (see Large *et al.*, 2005, for a discussion). Implicit in the term 'SEDEX' is that ore-forming fluids 'exhale' into the water column. The most recent comprehensive study of HYC (Ireland *et al.*, 2004) documents the relationship between sedimentary facies and ore distribution, and uses textural, geochemical and isotopic data to support a SEDEX model that invokes a sea floor brine pool and precipitation of Zn and Pb sulphides from the water column. Most alternative models for HYC (e.g., Williams, 1978) argue that Zn and Pb sulphides did not form in the water column, but rather a few centimetres or decimetres below the sea floor. In this case, ore fluids flow laterally for substantial distances within the unconsolidated sediments depositing Zn and Pb sulphides. However, although not explicit in sub-seafloor models, the 'spent' ore fluids would eventually escape into the overlying water column. The presence of broad primary dispersion haloes of Fe and other ore-fluid associated elements around HYC, and similar northern Australian deposits (Large *et al.*, 2005) indicates, regardless of the precise timing of ore formation, that there was a significant chemical contribution to basin waters by ore-forming hydrothermal fluids.

We collected samples of dolomitic shales and siltstones from six drill cores through the Barney Creek Fm (Table 1, Fig. 2, Fig. 3). and some of the over- and underlying dolomite units with varying distance from the HYC deposit. Previous work has demonstrated a progressive

decline in the hydrothermal fluid signal in the three most distal cores (20 km – MY4, 31 km – LY1, and 55 km – MBX1, Mukherjee & Large, 2017), while organic biomarker studies identified gradients in thermal maturity over shorter distances of several hundred meters from the HYC deposit (Chen *et al.*, 2003). Our sample set thus has the potential to detect both near and far-field effects. We express distances relative to the HYC deposit (Table 1), which is by far the largest deposit in the basin. We emphasize that our sampling strategy of focusing on primarily one geological unit (the Barney Creek Fm) minimizes the degree of differential diagenetic processes that are known to occur under differing redox conditions and sinking depths (Robinson *et al.*, 2012). As all our samples come from a relatively deep basinal setting with anoxic bottom waters, suitable for ore formation (see above), post-depositional diagenetic alteration of nitrogen isotopic ratios was likely minimal (< 1-2‰, Robinson *et al.*, 2012). Furthermore, all samples contain abundant host phases for authigenic nitrogen in the form of organic matter and clay minerals.

3. Methods

The interiors of the drill cores were hammered into mm-sized chips with a steel pestle on a steel plate and then cleaned sequentially with methanol, 1M HCl (both reagent grade) and DI-H_2O (18MΩ cm^{-1}) to remove surface contaminants. The chips were dried overnight in a closed oven at 60°C and then pulverized in an agate ball mill. The powder was decarbonated with two treatments of 2M HCl, washed three times with DI-H_2O, and dried again in the oven. Aliquots of the dry powder were weighed into 8 x 5 mm tin capsules and analysed with an EA IsoLink coupled via a ConFlo IV to a MAT253 isotope ratio mass spectrometer (Thermo Fisher Scientific). USGS-40 and USGS-41 were used for calibration. Isotopic data are expressed in standard delta notation ($\delta = [R_{sample}/R_{standard} - 1]$ x 1000), where $R = {}^{13}C/{}^{12}C$ for $\delta^{13}C$ and $R = {}^{15}N/{}^{14}N$ for $\delta^{15}N$. Standards are VPDB for carbon and atmospheric air for nitrogen. USGS-42 and USGS-62 were used as a quality control. For USGS-42, we obtained values of -21.07 ± 0.08 ‰ (1SD, n = 6) and +7.81 ± 0.16 ‰ for carbon and nitrogen isotopes, respectively, which are in good agreement with accepted values of -21.09 ± 0.10 ‰ and +8.05 ± 0.10 ‰. For USGS-62, which was measured for nitrogen only, we obtained a value of +20.21 ± 0.01 ‰ (n = 2), which also agrees well with the expected value of +20.17 ± 0.06 ‰. Following convention, ratios of total organic carbon (TOC) to total nitrogen (TN), hereafter C/N, are expressed in units of mol/mol.

4. Results

We did not observe any systematic trends in any of the parameters within the individual cores. However, the data as a whole (Table 2) reveal a broad covariance in $\delta^{15}N$ and C/N ratios with distance from the HYC ore body: $\delta^{15}N$ increases from a mean of +4.0 ± 0.4 ‰ in core F11/89 to +6.7 ± 0.7 ‰ in core MBX (Fig. 4a), while C/N ratios increase from 28 ± 1 to 56 ± 13 over the same interval (Fig. 4b). The two parameters are therefore weakly correlated (Fig. 5a) with r^2 = 0.20 for the whole dataset and r^2 = 0.58 after averaging the data for each core.

Across the whole dataset, TN correlates strongly with TOC (Fig. 6a, r^2 = 0.96). A close-up view of the samples with lower TN and TOC contents shows that the trend lines for each core are slightly offset from each other, *i.e.* they have differing slopes (Fig. 6b), owing to their differing C/N ratios. Overall, intercepts on the TN-axis are less than 105 µg/g (core LY1 shows a negative intercept of -13 µg/g, but this value changes to 18 µg/g if one anomalous data point is excluded). Core F11/89, which is closest to the ore body, has the smallest TN-axis intercept with 5.5 µg/g,

but there is otherwise no systematic covariance between intercepts and distance from the ore. Organic carbon isotopes do not show any trend with distance (Fig. 3, Fig. 5b). Overall, $\delta^{13}C$ values cluster around a mean of -32.7 ± 0.7 ‰ and show no covariance with nitrogen isotopes, C/N ratios or TOC (r^2 always < 0.04).

5. Discussion

5.1. Metamorphism and Thermal Alteration

Both nitrogen and carbon isotopes can be altered during metamorphism. Heating may lead to partial volatilization of these elements with a preference for the lighter isotopes, such that the residual organic matter develops progressively increasing $^{15}N/^{14}N$ and $^{13}C/^{12}C$ ratios (Haendel *et al.*, 1986; Schidlowski, 1987). However, these effects are small (< 1-2 ‰) below greenschist facies. The McArthur Group in the sampled area is essentially unmetamorphosed, meaning that regional metamorphic effects are unlikely to have perturbed the measured isotopic ratios. In fact, the Barney Creek Fm is known for its exceptionally low metamorphic grade that has allowed the preservation of organic biomarkers (Brocks *et al.*, 2005; Lee & Brocks, 2011; Holman *et al.*, 2014). However, increasing thermal degradation of organic compounds has been recognized closer to the HYC ore body, likely caused by the direct influence of hydrothermal fluids (Williford *et al.*, 2011; Holman *et al.*, 2014). It is therefore conceivable that the observed trends in our data with distance from the ore body (Fig. 4) are the relic of a hydrothermal alteration gradient. However, the alteration by hot fluids tends to mobilize nitrogen preferentially to carbon from organic matrices with no significant isotopic effect (< 1 ‰) to either $\delta^{15}N$ or $\delta^{13}C$ (Ader *et al.*, 1998; Schimmelmann *et al.*, 2001; Ader *et al.*, 2006; Boudou *et al.*, 2008). The observed decrease in $\delta^{15}N$ and C/N ratios closer to the ore body can therefore not be explained by secondary alteration of primary organic matter via hot fluids. We stress that metamorphic alteration of sedimentary rocks can cause an isotopic divergence in $\delta^{15}N$ between kerogen- and silicate-bound ammonium, and this effect may be enhanced in the presence of hydrothermal fluids (reviewed by Stüeken *et al.*, 2017), but this process is not known to lead to a net decrease in bulk rock $\delta^{15}N$ values. Therefore, the isotopic trend with distance from the HYC deposit is most likely a signature of primary environmental processes. Our data would thus be consistent with our hypothesis that the biogeochemical nitrogen cycle was distinct in the proximity of hydrothermal vents compared to the open ocean.

5.2. Hydrothermally Sourced Bioavailable Nitrogen

Modern hydrothermal vents host diverse microbial communities that take advantage of metabolites provided by submarine volcanism, such as hydrogen, transition metals or sulphur. With regards to nitrogen, it has been noticed that hydrothermal vents can be enriched in dissolved ammonium if the hydrothermal fluids circulate through sediment packages prior to venting into the open ocean (Lilley *et al.*, 1993). Sediments and sedimentary rocks are highly enriched in nitrogen relative to igneous rock, especially if they contain organic matter (Johnson & Goldblatt, 2015). Hot fluids with temperatures of 200-300°C circulating through sedimentary strata can therefore entrain nitrogen in the form of ammonium (Ader *et al.*, 1998; Ader *et al.*, 2006; Boudou *et al.*, 2008). Some modern vents reach millimolar concentrations of ammonium (Lilley *et al.*, 1993), which is 2-3 orders of magnitude higher than background levels of dissolved nitrate in the modern ocean. Studies of modern vents and seeps suggest biological uptake of ammonium from

hydrothermal fluids (e.g., Feng *et al.*, 2015). Mississippian-age organic-rich siliceous black shales of the Kuna Formation in northwest Alaska, which are the host rocks to the supergiant Red Dog SEDEX Zn deposit, are reported to contain ammonium enrichments in clay minerals sourced from hydrothermal fluids (Sterne *et al.*, 1984). Although hydrothermal nitrogen cycling in the Proterozoic ocean has to our knowledge not been thoroughly investigated, our data from the McArthur Group are most parsimoniously explained by a similar mechanism whereby hydrothermally-sourced fixed nitrogen (ammonium or nitrate) was assimilated into microbial biomass or into illite clays (but see section 5.3).

Recent genetic models for the HYC deposit suggest that hydrothermal fluids travelled upwards for around 10 km along the Emu Fault before reaching the now mineralized horizon in the Barney Creek Fm (Rawlings *et al.*, 2004; Kunzmann *et al.*, 2019). The fluids thus passed through a large proportion of the underlying Tawallah Group, which includes thick sedimentary red beds and minor organic-rich horizons. Previous studies identified polycyclic aromatic hydrocarbons (PAHs) within and proximal to the HYC mineralization (Chen *et al.*, 2003; Williford *et al.*, 2011), and isotopic data suggest that these hydrocarbons were derived from the Wollogorang Fm in the Tawallah Group (Williford *et al.*, 2011). This unit, dated to 1730 ± 4 Ma, is a 20 m thick dolomitic black shale with up to 6 wt. % TOC (Donnelly & Jackson, 1988). Enrichments in sulphur and base metals indicate the passage of hot, mineralizing fluids through these strata (Donnelly & Jackson, 1988; Spinks *et al.*, 2016). Given that hot fluids are known to dislodge ammonium from organic matter (Boudou *et al.*, 2008), we speculate that these hydrothermal fluids did not just assimilate hydrocarbons but also fixed nitrogen from the black shales of the Wollogorang Fm. Hydrothermal transport of this nitrogen, as either ammonium or nitrate, from the Wollogorang Fm to the Barney Creek sub-basin could thus plausibly explain the relatively low C/N ratios (*i.e.,* relative N enrichment) and distinct isotopic ratios close to the ore body. Importantly, it is thought that these fluids were sufficiently oxidized to carry sulphate (Cooke *et al.*, 1998), and therefore also ammonium may have undergone oxidation to nitrate within the fluid prior to seeping into the anoxic Barney Creek sub-basin where it was re-reduced and re-assimilated into biomass. While this interpretation of nitrogen transport from the Wollogorang Fm to the Barney Creek basin is speculative and would require additional tests, it is consistent with our hypothesis that hydrothermal fluid circulation can recycle fixed nitrogen from sediments back into the water column, which may have locally offset the lack of aerobic biomass remineralization prior to sediment deposition (Kipp & Stüeken, 2017).

5.3. Hydrothermal nitrogen uptake into biomass

If correct, our interpretation of a hydrothermal nitrogen source leaves open the question of how the dissolved ammonium or nitrate was trapped in the Barney Creek Fm. Two endmember possibilities have to be considered: (a) If the nitrogen was in the form of ammonium, then it may have become incorporated into phyllosilicate minerals, as is commonly the case in diagenetic settings (Schroeder & McLain, 1998). NH_4^+ has a similar ionic radius and the same charge as K^+ and therefore substitutes into potassic clays. (b) Alternatively, the fixed nitrogen (ammonium or nitrate) may have become incorporated into organic matter by microbes that were utilizing it as a nutrient. A combination of both option is also possible. In the case of option (a), we would expect to see a large enrichment in TN relative to TOC proximal to the ore body, as is the case around the Mississippian Red Dog SEDEX deposit in Alaska (Sterne *et al.*, 1984). In this case, ammonium thus appears to have been trapped in clay minerals. In the case of the Barney Creek Formation,

C/N ratios are indeed lower closer to the ore (Fig. 4b); however, the data do not show a significant intercept on the TN axis, *i.e.,* the TN-axis intercept is equal to less than 10% of the TN content of almost all samples in the two most proximal cores (Fig. 6b), suggesting that most N in these rocks is directly derived from organic matter (option b). Some of it may reside in phyllosilicate minerals today, due to biomass degradation, diagenetic release of ammonium into porewaters, and uptake into secondary illite phases (Schroeder & McLain, 1998). However, the lack of excess amounts of TN relative to TOC probably rules out additional N incorporation into clay minerals during or after the time of sediment deposition. In contrast, the host rocks of the Mississippian Red Dog SEDEX deposit display a TN intercept of 1200 µg/g, indicating a significant clay-bound N fraction in that case (Sterne *et al.*, 1984).

For comparison, data from the modern Black Sea and the Eocene Monterey basin, two restricted anoxic settings, have much higher intercepts of 570 µg/g and 3000 µg/g (Calvert, 2001; Fulton *et al.*, 2012). The water column of the Black Sea is enriched in ammonium at depth with concentrations up to 100 µM (Brewer & Murray, 1973) because of strong density stratification. This scenario can lead to significant adsorption of ammonium to clay minerals (Boatman & Murray, 1982). In contrast, samples from the modern Atlantic and the Labrador Sea, two well-ventilated settings where dissolved nitrogen is quantitatively consumed by primary producers, show TN-axis intercepts of roughly 25 µg/g and 37 µg/g, respectively (Macko & Pereira, 1990; Muzuka & Hillaire-Marcel, 1999). These values are closer to those observed in the McArthur Group (Fig. 6b). Of course, modern ventilated settings are fully oxygenated and contain nitrate rather than ammonium, but in any case, they provide an example of a scenario where all sedimentary N that gets archived in the sedimentary record is derived from the burial and degradation of organic matter rather than adsorption of ammonium to clay particles within the water column. We therefore conclude that the tight correlation between TN and TOC and the relatively small TN-axis intercepts indicate that most of the nitrogen was introduced into the rocks in an organic-bound form rather than as exogenous adsorbed or detrital ammonium.

5.4. Productivity hotspots?

If this model is correct, then the relatively lower C/N ratios proximal to the ore are perhaps reflecting greater N availability near the discharge zone, allowing organisms to uptake more N into their biomass. It is unlikely that the measured C/N ratios reflect the exact initial composition of biomass (*i.e.*, its Redfield ratio), because diagenesis and biomass degradation would later have led to preferential N loss relative to C. However, if all sites experienced similar post-depositional regional metamorphism, then the *relative* difference in measured C/N ratios may reflect *relative* initial differences. While complex algae have tightly controlled C/N ratios around 6-7, some prokaryotic organisms have much more flexible biochemistries that can adapt to changing nutrient supplies (Geider & La Roche, 2002; Planavsky, 2014). This flexibility is achieved by changing the proportion of proteins relative to lipids and nucleic acids within cells (Geider & La Roche, 2002). Our data may therefore provide tentative evidence that nitrogen-rich hydrothermal effluents in the McArthur Basin created niches for organisms to thrive in nutrient-replete conditions under which the production of cellular N storage was favoured. We note that TOC levels in the most proximal core are similar to or lower than in more distal cores (Fig. 3), but they are still on the order of 1 wt. %, which is a significant amount. Furthermore, it is important to consider that the hydrothermal vent environment would have been characterised by high salinity and elevated temperature, thus selecting for extremophilic organisms. It is also possible that some fraction of

the hydrothermally-sourced ammonium or organic-bound nitrogen along with other nutrient elements was transported further into the basin to fuel biological productivity in more distal, environmentally less extreme settings, possibly accounting for elevated TOC levels in the more distal drill cores.

Nitrogen isotopes can provide additional information about metabolic processes (see Stüeken *et al.*, 2016 and references therein). Nitrogen enters the biosphere through biological fixation of N_2 into intracellular ammonium, which gets released during biomass degradation. This process produces dissolved NH_4^+ with an isotopic composition of around -1‰ on average. In the presence of nanomolar levels of O_2, NH_4^+ is rapidly oxidized to NO_3^-, which can in turn undergo reduction to N_2 gas (denitrification, or anammox if coupled to NH_4^+ oxidation) under suboxic conditions. The net effect is loss of isotopically light nitrogen from the system, rendering the residual NO_3^- isotopically heavy. In the modern ocean, for example, dissolved NO_3^- has a composition of around +5‰, and this composition can become archived in sediments, if primary producers uptake nitrate into their cells and get buried. Nitrate uptake is usually near-quantitative, but it can impart a fractionation of 5-10‰ in favour of ^{14}N if nitrate is supplied in excess. Elevated $\delta^{15}N$ values in the sedimentary rock record are therefore usually taken as evidence for a redox-active nitrogen cycle during the time of deposition. In the absence of free O_2, dissolved nitrogen remains in the form of ammonium, and biological assimilation of ammonium favours the light isotope with a large fractionation of 4-27‰, leading to low $\delta^{15}N$ values in biomass and higher values in residual dissolved ammonium. However, if assimilation goes to completion, then this fractionation is not expressed, such that living organisms preserve the isotopic composition of the ammonium source.

In the case of the McArthur Group, we cannot be certain if the fixed nitrogen contained in the hydrothermal fluid was in the form of ammonium or nitrate. Values around +4‰ have been reported from the Wollogorang Fm (Yoshiya *et al.*, 2015), which is the most likely nitrogen source. Hence, the tight cluster of $\delta^{15}N$ values around +4‰ close to the ore body in the Barney Creek Fm (Fig. 4a) may suggest that either (a) biological uptake of nitrogen from the hydrothermal fluid was quantitative with no net isotopic fractionation, or (b) uptake was non-quantitative, but the isotopic fractionation associated with microbial uptake was relatively small. If we are correctly interpreting the low C/N ratios in the most proximal cores as evidence of a high nitrogen supply, then a low isotopic fractionation factor during biological uptake is perhaps the most likely explanation. This would suggest that the fluids were carrying nitrate into the Barney Creek basin, because the isotopic fractionation associated with partial nitrate assimilation is much smaller than that of ammonium assimilation (see above). If, for example, 80% of the injected nitrate were assimilated, the resulting biomass would be 1.2-2.5‰ offset from the nitrate source. Such as small offset would be consistent with natural uncertainty in the data. However, we stress that we cannot rule out ammonium as the major nitrogen phase at this point, which would then require quantitative uptake by vent biota to explain our isotopic data.

More distal to the HYC deposit, where $\delta^{15}N$ values reach up to +7.5‰, the nitrogen cycle may have been more strongly affected by non-quantitative redox reactions. As noted above, systematically positive values indicate loss of isotopically light nitrogen from the system, which is usually attributed to partial denitrification or anammox along a redoxcline (Stüeken *et al.*, 2016). Previous studies of the Barney Creek Fm have revealed anoxic ferruginous (Planavsky *et al.*, 2011) and possibly locally euxinic (H_2S-rich) bottom waters in this basin, which probably played a pivotal role in the formation of the ore deposit (Holman *et al.*, 2014). In contrast, surface waters in the mid-Proterozoic were likely well oxygenated (Steadman *et al.*, 2020). Denitrification could

have proceeded along this redox interface. Potential sources of nitrate could have been (a) remineralisation of biomass that formed and thrived in the oxic photic zone of the basin, and/or (b) upwelling of residual, isotopically enriched nitrate from the hydrothermal fluids, or (c) upwelling and oxidation of organic-bound nitrogen that formed from biological uptake of hydrothermal ammonium in the deeper water column. The two latter options would imply that some of the hydrothermally-source nitrogen was dispersed further into the basin. If that was the case, then hydrothermal nutrient supplies, including fixed nitrogen, may have fuelled primary and secondary productivity and the accumulation of organic matter in sediments throughout the McArthur Basin (Fig. 7).

6. Conclusions

Modern hydrothermal fluids are known to recycle fixed nitrogen from sediments back into the water column (Lilley *et al.*, 1993), and our data from the Barney Creek Fm support our hypothesis that this recycling process may also have operated in the Proterozoic. The relatively low C/N ratios closer to the ore deposit (Fig. 4b), paired with low TN intercepts in TN versus TOC scatter plots (Fig. 6a, 6b) and a tight cluster in $\delta^{15}N$ ratios (Fig. 4a, 5a), would be consistent with the interpretation of a hydrothermal source of fixed nitrogen that was largely assimilated into biomass. Spatial gradients suggest that the direct influence of hydrothermal N input extended for a few kilometres around the vent, but it is conceivable that some organic-bound nitrogen or nitrate was exported further, leading to elevated productivity across the basin (Fig. 7). The nitrogen contained in hydrothermal fluids was probably derived from the underlying Wollogorang Fm, which has previously been identified as a source of hydrocarbons to the hydrothermal fluid (Williford *et al.*, 2011). Hot fluids interacting with organic matter are known to entrain ammonium with no detectable isotopic fractionation (Boudou *et al.*, 2008). The locality of hydrothermal venting during the deposition of the Barney Creek Fm thus perhaps allowed organisms to thrive in an ammonium-rich environment.

It has previously been proposed that the stoichiometry of marine life evolved over Earth history (Planavsky, 2014). For example, microbial C/N ratios may have been substantially higher in the distant past when fixed nitrogen concentration in seawater were probably low. Sedimentary exhalative hydrothermal systems, such as in the HYC deposit, that provided point source of fixed nitrogen into the ocean may have created niches for early life to build up a higher cellular protein content (Geider & La Roche, 2002). Sedimentary exhalative ore deposits are common in the Proterozoic rock record, and so it is conceivable that these systems created important habitats for early biological evolution.

Acknowledgements

Tables

Table 1: Drill core localities

Full name	Abbreviation	Distance from HYC [km]	Geographic location (MGA94-Zone53)		Structural sub-basin
			Easting (m)	Northing (m)	
MBXDD001	MBX	60	606036	8121952	Gorge
Leila Yard 1	LY1	31	592608	8163118	Leila Creek
Myrtle 4	MY4	20	612912	8164181	Myrtle
Barney Creek 3	BC3	15	605500	8174500	Barney Creek
Homestead 6	HS6	4	616000	8179000	HYC
F11/98	F11/98	Fringe ore	617000	8181600	HYC

Table 2: Carbon and nitrogen data from this study. TOC = total organic carbon; TN = total nitrogen. All parameters were measured on decarbonated sample aliquots.

Depth [m]	TN [μg/g]	$\delta^{15}N$ [‰]	TOC [wt. %]	$\delta^{13}C$ [‰]	C/N [mol/mol]
MBX:					
30.1	249	6.11	0.93	-33.24	44
47.5	146	7.53	0.55	-33.38	44
70.2	259	6.21	0.97	-33.81	44
81.9	2039	6.83	12.98	-32.86	74
100.7	1660	7.00	9.50	-33.19	67
118.3	428	5.95	2.00	-34.00	54
128.4	1690	7.47	9.79	-33.29	68
LY1:					
335	183	6.75	0.64	-32.30	41
337	264	6.89	1.49	-32.76	66
342	304	6.31	1.87	-31.99	72
367	86	5.42	0.75	-31.36	101
382.8	329	6.19	1.48	-33.08	52
386	189	5.95	0.79	-32.68	49
398.1	242	5.27	1.26	-32.56	61
407.5	411	5.52	2.12	-31.58	60
424.5	588	5.40	2.51	-31.35	50
MY4:					
17.5	217	5.74	0.69	-32.65	37
26.2	615	5.74	2.24	-31.61	43
32.8	188	5.63	0.61	-31.50	38
44.8	218	5.95	0.69	-31.36	37
84.4	679	6.31	3.57	-33.27	61
85.2	266	6.35	1.46	-33.38	64
88.4	89	5.89	0.07	-32.65	10
91.8	66	7.45	0.23	-33.04	41
BC3:					
157	387	5.13	1.66	-31.32	50
165	296	4.58	0.96	-32.08	38
213.4	239	4.71	1.04	-32.58	51
250.7	359	4.71	1.22	-32.67	40
286.1	270	4.68	1.01	-33.17	44
HS6:					
80	347	5.11	0.94	-33.30	32
112	773	5.96	2.19	-32.95	33

140	343	5.07	0.92	-33.58	31
151.7	354	4.76	1.00	-33.22	33
171.7	245	4.54	0.61	-33.28	29
F11/98:					
39.7	387	4.54	0.91	-33.30	28
84.7	296	4.03	0.68	-33.21	27
94.7	312	3.83	0.78	-32.69	29
134.7	250	3.77	0.60	-32.67	28

Figures
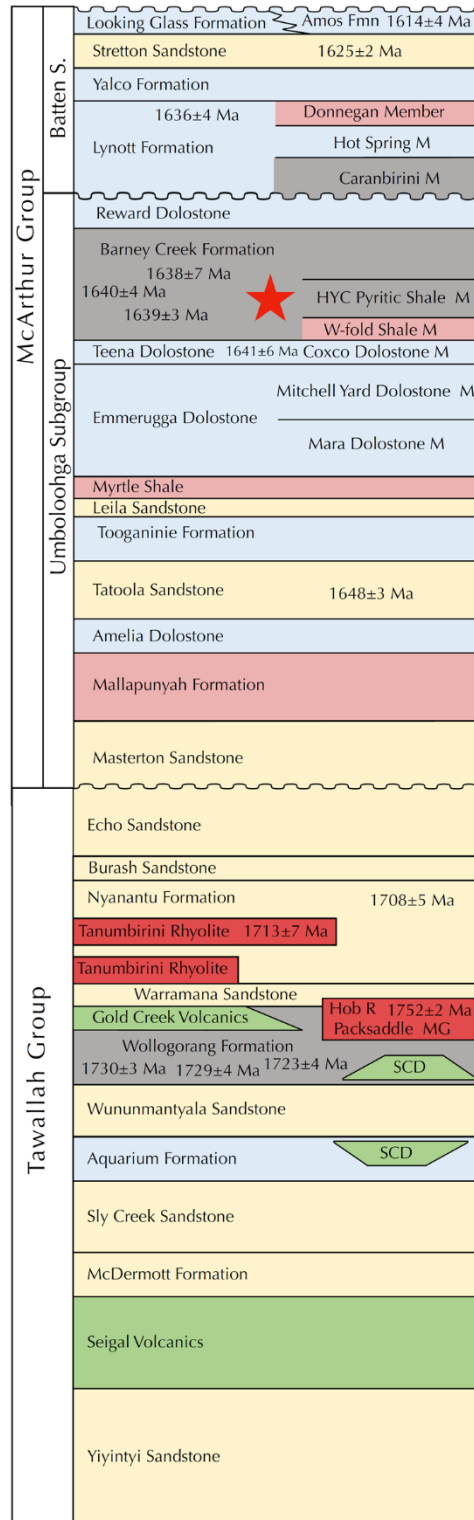
Figure 1: Lithostratigraphy of late Paleoproterozoic sequences from the southern McArthur Basin (see Ahmad *et al.*, 2013 for details). The labelled boxes are scaled to approximate relative thickness

of individual units and coloured according to the dominant lithology (blue - carbonate; yellow - sandstone; pink - oxidised clastics; grey - reduced shales and siltstones; red - felsic volcanics and intrusive equivalents; green - mafic volcanics and high-level intrusives). Radiometric ages from the sedimentary units are SHRIMP U-Pb ages of juvenile detrital zircons populations (Southgate *et al.*, 2000, and references therein). (Red star indicates the stratigraphic position of the HYC deposit; MG = microgranite; M = Member).
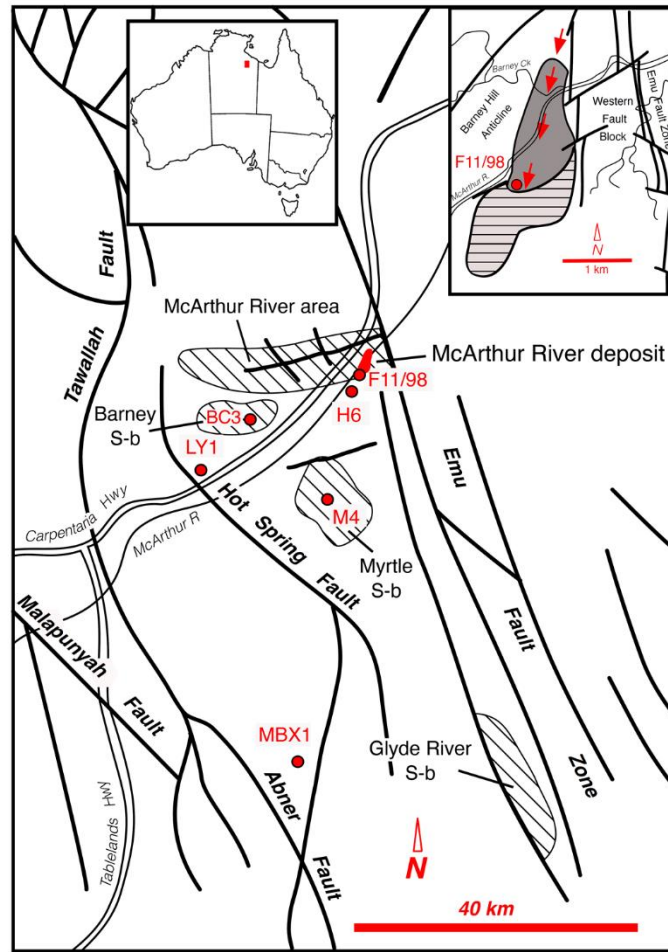
Figure 2: Map of an area around McArthur River Mine in the Northern Territory showing the locations of six drill-cores sampled for this study. Major fault structures and several 'sub-basins' (Pietsch *et al.*, 1991) are highlighted. Note the 'McArthur River area' encompasses several small 'sub-basins' and the recently discovered Teena Zn-Pb-Ag deposit (Taylor *et al.*, 2017). The inset (modified from Ireland *et al.*, 2004 and references therein) shows the 'footprint' of high-grade stratiform HYC mineralization (solid grey) and the distribution of nodular carbonate-bearing, low-Zn grade mineralization (lighter-hatched area to the south). Red arrows are the inferred direction of flow of Zn-Pb (and N) -bearing ore fluids. See text for further discussion.
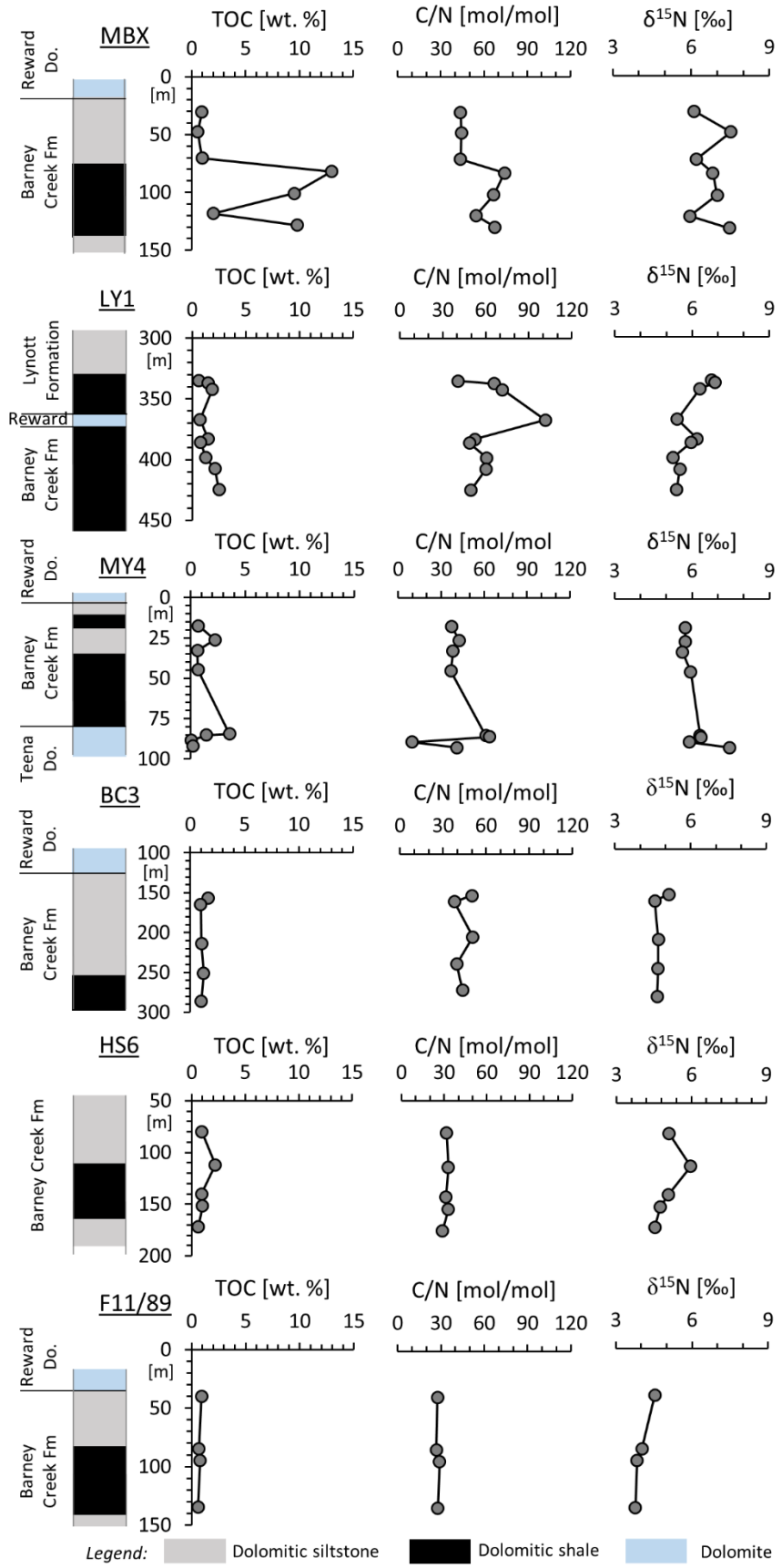
Legend: ▢ Dolomitic siltstone   ▮ Dolomitic shale   ▢ Dolomite

Figure 3: Stratigraphy of the six drill cores sampled in this study, sorted from closest to the ore at the bottom to furthest away at the top.
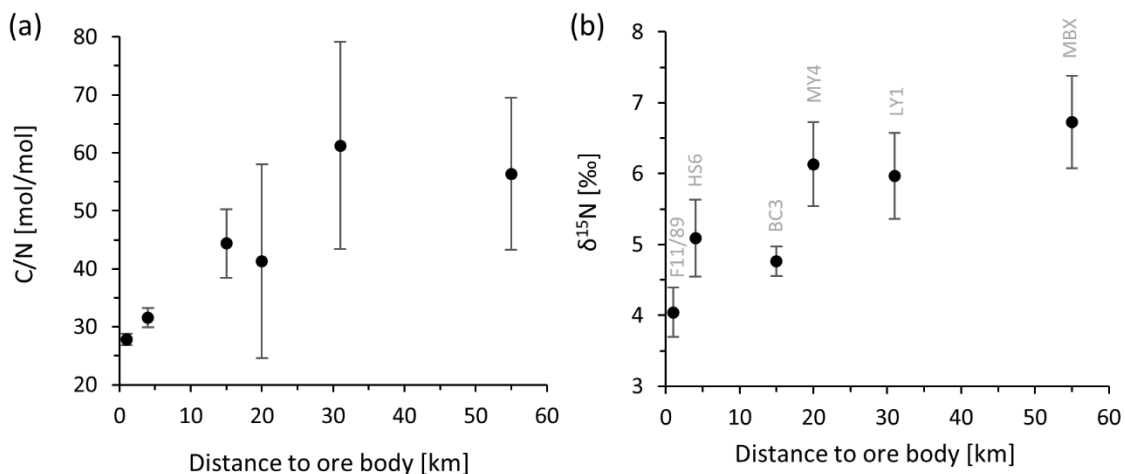

Figure 4: (a) Total organic carbon to total nitrogen ratios (C/N) versus distance from the ore body. (b) Bulk nitrogen isotope ratios versus distance from the ore body. Each point marks the average of all data from one drill core with the marked distance (Table 1). Error bars are 1SD around the mean of data points from each core.
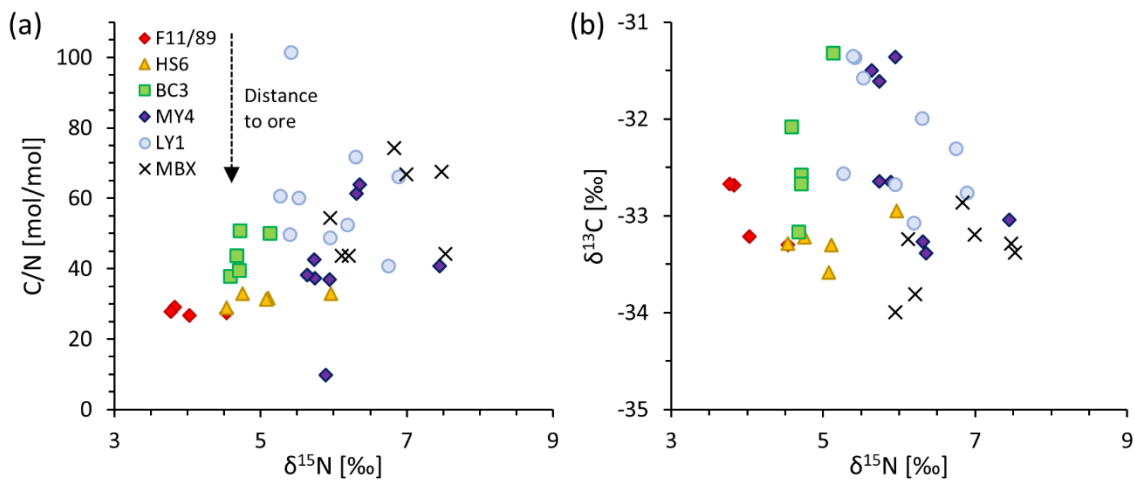

Figure 5: (a) Total organic carbon to total nitrogen ratios (C/N) versus bulk nitrogen isotopes. Data reveal a trend with lower C/N and $\delta^{15}N$ values closer to the ore. (b) Organic carbon versus bulk nitrogen isotopes, showing no trend with distance in $\delta^{13}C$.
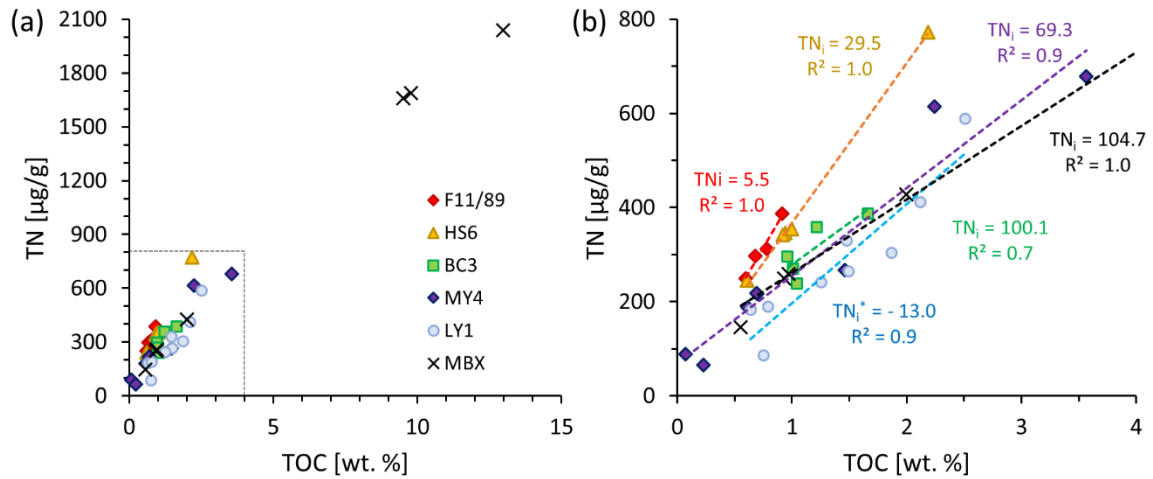
Figure 6: Total nitrogen (TN) versus total organic carbon (TOC) for all data (a) and for those below 800 µg/g TN and 4 wt. % TOC (b). In panel (b), correlation coefficients and TN axis intercepts (TN_i) of linear trendlines are shown. TN axis intercepts are in units of µg/g. *For core LY1, the intercept increases from -13 to +18 if the most N-depleted data point is excluded.
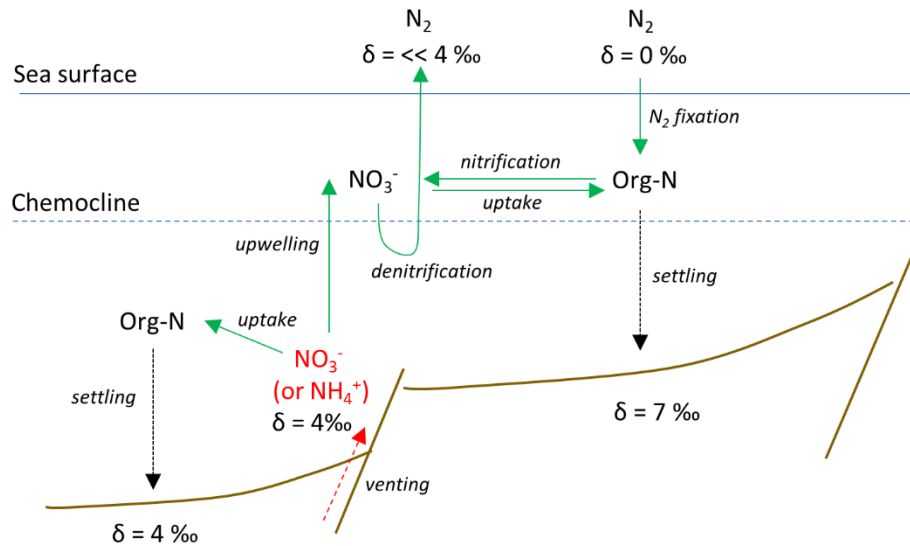

Figure 7: Schematic of the inferred nitrogen cycle in the McArthur Basin. NH_4^+ is introduced along faults together with mineralising fluids. Waters below the chemocline are anoxic while surface waters are oxygenated. Most hydrothermally-source NH_4^+ is assimilated into biomass, but via remineralization, upwelling and nitrification some of the NH_4^+ may be transported into the surface ocean.

17

References

Ader M, Boudou J-P, Javoy M, Goffe B, Daniels E (1998) Isotope study on organic nitrogen of Westphalian anthracits from the Western Middle field of Pennsylvania (USA) and from the Bramsche Massif (Germany). *Organic Geochemistry,* **29**, 315-323.

Ader M, Cartigny P, Boudou J-P, Oh J-H, Petit E, Javoy M (2006) Nitrogen isotopic evolution of carbonaceous matter during metamorphism: methodology and preliminary results. *Chemical Geology,* **232**, 152-169.

Ahmad M, Dunster JN, Munson TJ (2013) McArthur Basin. *Special Publication-Northern Territory Geological Survey,* **5**, 1-15.

Ardyna M, Lacour L, Sergi S, d'Ovidio F, Sallée JB, Rembauville M, Blain S, Tagliabue A, Schlitzer R, Jeandel C, Arrigo KR (2019) Hydrothermal vents trigger massive phytoplankton blooms in the Southern Ocean. *Nature Communications,* **10**, 1-8.

Betts PG, Giles D (2006) The 1800–1100 Ma tectonic evolution of Australia. *Precambrian Research,* **144**, 92-125.

Boatman CD, Murray JW (1982) Modeling exchangeable NH_4^+ adsorption in marine sediments: Process and controls of adsorption. *Limnology and Oceanography,* **27**, 99-110.

Boudou JP, Schimmelmann A, Ader M, Mastalerz M, Sebilo M, Gengembre L (2008) Organic nitrogen chemistry during low-grade metamorphism. *Geochimica et Cosmochimica Acta,* **72**, 1199-1221.

Brewer PG, Murray JW (1973) Carbon, nitrogen and phosphorus in the Black Sea. *Deep Sea Research and Oceanographic Abstracts* **20**, 803-818.

Brocks JJ, Love GD, Summons RE, Knoll AH, Logan GA, Bowden SA (2005) Biomarker evidence for green and purple sulphur bacteria in a stratified Palaeoproterozoic sea. *Nature,* **437**, 866-870.

Bull SW (1998) Sedimentology of the Palaeoproterozoic Barney Creek formation in DDH BMR McArthur 2, southern McArthur basin, northern territory. *Australian Journal of Earth Sciences,* **45**, 21-31.

Calvert S (2001) *The Monterey Formation: From Rocks to Molecules,* Columbia University Press, New York.

Chen J, Walter MR, Logan GA, Hinman MC, Summons RE (2003) The Paleoproterozoic McArthur River (HYC) Pb/Zn/Ag deposit of northern Australia: organic geochemistry and ore genesis. *Earth and Planetary Science Letters,* **210**, 467-479.

Cooke DR, Bull SW, Donovan S, Rogers JR (1998) K-metasomatism and base metal depletion in volcanic rocks from the McArthur Basin, Northern Territory; implications for base metal mineralization. *Economic Geology,* **93**, 1237-1263.

Crockford PW, Hayles JA, Bao H, Planavsky NJ, Bekker A, Fralick PW, Halverson GP, Bui TH, Peng Y, Wing BA (2018) Triple oxygen isotope evidence for limited mid-Proterozoic primary productivity. *Nature,* **559**, 613-616.

Donnelly TH, Jackson MJ (1988) Sedimentology and geochemistry of a mid-Proterozoic lacustrine unit from northern Australia. *Sedimentary Geology,* **58**, 145-169.

Feng D, Cheng M, Kiel S, Qiu JW, Yang Q, Zhou H, Peng Y, Chen D (2015) Using Bathymodiolus tissue stable carbon, nitrogen and sulfur isotopes to infer biogeochemical process at a cold seep in the South China Sea. *Deep Sea Research Part I: Oceanographic Research Papers,* **104**, 52-59.

Fulton JM, Arthur MA, Freeman KH (2012) Black Sea nitrogen cycling and the preservation of phytoplankton δ^{15}N signals during the Holocene. *Global Biogeochemical Cycles,* **26**.

Geider R, La Roche J (2002) Redfield revisited: variability of C:N:P in marine microalgae and its biochemical basis. *European Journal of Phycology,* **37**, DOI: 10.1017/S0967026201003456.

Haendel D, Muehle K, Nitzsche H-M, Stiehl G, Wand U (1986) Isotopic variations of the fixed nitrogen in metamorphic rocks. *Geochimica et Cosmochimica Acta,* **50**, 749-758.

Holman AI, Grice K, Jaraula CM, Schimmelmann A (2014) Bitumen II from the Paleoproterozoic Here's Your Chance Pb/Zn/Ag deposit: Implications for the analysis of depositional environment and thermal maturity of hydrothermally-altered sediments. *Geochimica et Cosmochimica Acta,* **139**, 98-109.

Ireland T, Large RR, McGoldrick P, Blake M (2004) Spatial distribution patterns of sulfur isotopes, nodular carbonate, and ore textures in the McArthur River (HYC) Zn-Pb-Ag deposit, Northern Territory, Australia. *Economic Geology,* **99**, 1687-1709.

Johnson B, Goldblatt C (2015) The Nitrogen budget of Earth. *Earth-Science Reviews,* **148**, 150-173.

Kipp MA, Stüeken EE (2017) Biomass recycling and Earth's early phosphorus cycle. *Science Advances,* **3**, doi: 10.1126/sciadv.aao4795.

Knoll AH, Nowak MA (2017) The timetable of evolution. *Science Advances,* **3**, doi: 10.1126/sciadv.1603076.

Koehler MC, Stüeken EE, Kipp MA, Buick R, Knoll AH (2017) Spatial and temporal trends in Precambrian nitrogen cycling: a Mesoproterozoic offshore nitrate minimum. *Geochimica et Cosmochimica Acta,* **198**, 315-337.

Kunzmann M, Schmid S, Blaikie TN, Halverson GP (2019) Facies analysis, sequence stratigraphy, and carbon isotope chemostratigraphy of a classic Zn-Pb host succession: The Proterozoic middle McArthur Group, McArthur Basin, Australia. *Ore Geology Reviews,* **106**, 150-175.

Large RR, Bull SW, McGoldrick PJ, Walters SG (2005) Stratiform and strata-bound Zn-Pb-Ag deposits in Proterozoic sedimentary basins, northern Australia. *Economic Geology,* **100**, 931-963.

Lee C, Brocks JJ (2011) Identification of carotane breakdown products in the 1.64 billion year old Barney Creek Formation, McArthur Basin, northern Australia. *Organic Geochemistry,* **42**, 425-430.

Lilley MD, Butterfield DA, Olson EJ, Lupton JE, Macko SA, McDuff RE (1993) Anomalous CH4 and NH4+ concentrations at an unsedimented mid-ocean-ridge hydrothermal system. *Nature,* **364**, 45-47.

Macko SA, Pereira CPG (1990) Neogene paleoclimate development of the Antarctic Weddell Sea region: Organic geochemistry. In: *Proceedings Ocean Drilling Program, Scientific Results* (ed Barker PF). Ocean Drilling Program, College Station, TX, pp. 881-897.

McGoldrick P, Winefield P, Buli S, Selley D, Scott R (2010) Sequences, synsedimentary structures, and sub-basins: the where and when of SEDEX zinc systems in the southern McArthur basin, Australia. *Society of Economic Geologists, Special Publication,* **15**, 367-389.

Mukherjee I, Large R (2017) Application of pyrite trace element chemistry to exploration for SEDEX style Zn-Pb deposits: McArthur Basin, Northern Territory, Australia. *Ore Geology Reviews,* **81**, 1249-1270.

Mukherjee I, Large RR, Corkrey R, Danyushevsky LV (2018) The boring billion, a slingshot for complex life on Earth. *Scientific Reports,* **8**, doi: 10.1038/s41598-41018-22695-x.

Muzuka AN, Hillaire-Marcel C (1999) Burial rates of organic matter along the eastern Canadian margin and stable isotope constraints on its origin and diagenetic evolution. *Marine Geology,* **160**, 251-270.

Pietsch BA, Rawlings DJ, Creaser RA, Kruse PD, Ahmad M, Ferenczi PA, Findhammer TLR (1991) *Bauhinia Downs SE53-3,* Government Printer of the Northern Territory, Australia.

Planavsky NJ (2014) The elements of marine life. *Nature Geoscience,* **7**, 855-856.

Planavsky NJ, McGoldrick P, Scott CT, Li C, Reinhard CT, Kelly AE, Chu X, Bekker A, Love GD, Lyons TW (2011) Widespread iron-rich conditions in the mid-Proterozoic ocean. *Nature,* **477**, 448-451.

Rawlings DJ, Korsch RJ, Goleby BR, Gibson GM, Johnstone DW, Barlow M (2004) The 2002 southern McArthur Basin seismic reflection survey. *Geoscience Australia, Record,* **17**, 1-78.

Reinhard CT, Planavsky NJ, Gill BC, Ozaki K, Robbins LJ, Lyons TW, Fischer WW, Wang C, Cole DB, Konhauser KO (2017) Evolution of the global phosphorus cycle. *Nature,* **541**, 386-389.

Robinson RS, Kienast M, Albuquerque AL, Altabet M, Contreras S, De Pol Holz R, Dubois N, Francois R, Galbraith E, Shu T-C, Ivanochko T, Jaccard S, Kao S-J, Kiefer T, Kienast S, Lehmann M, Martinez P, McCarthy M, Moebius J, Pedersen T, Quan TM, Ryabenko E, Schmittner A, Schneider R, Schneider-Mor A, Shigemitsu M, Sinclair D, Somes C, Studer A, Thunell R, Yang J-Y (2012) A review of nitrogen isotopic alteration in marine sediments. *Paleoceanography,* **27**, doi: 10.1029/2012PA002321.

Schidlowski M (1987) Application of stable carbon isotopes to early biochemical evolution on Earth. *Annual Review of Earth and Planetary Sciences,* **15**, 47-72.

Schimmelmann A, Boudou JP, Lewan MD, Wintsch RP (2001) Experimental controls on D/H and $^{13}C/^{12}C$ ratios of kerogen, bitumen and oil during hydrous pyrolysis. *Organic Geochemistry,* **32**, 1009-1018.

Schine CM, Alderkamp AC, van Dijken G, Gerringa LJ, Sergi S, Laan P, van Haren H, van de Poll WH, Arrigo KR (2021) Massive Southern Ocean phytoplankton bloom fed by iron of possible hydrothermal origin. *Nature Communications,* **12**, 1-11.

Schroeder PA, McLain AA (1998) Illite-smectites and the influence of burial diagenesis on the geochemical cycling of nitrogen. *Clay Minerals,* **33**, 539-546.

Southgate PN, Bradshaw BE, Domagala J, Jackson MJ, Idnurm M, Krassay AA, Page RW, Sami TT, Scott DL, Lindsay JF, McConachie BA (2000) Chronostratigraphic basin framework for Palaeoproterozoic rocks (1730–1575 Ma) in northern Australia and implications for base-metal mineralisation. *Australian Journal of Earth Sciences,* **47**, 461-483.

Spinks SC, Schmid S, Pagés A, Bluett J (2016) Evidence for SEDEX-style mineralization in the 1.7 Ga Tawallah Group, McArthur Basin, Australia. *Ore Geology Reviews,* **76**, 122-139.

Steadman JA, Large RR, Blamey NJ, Mukherjee I, Corkrey R, Danyushevsky LV, Maslennikov V, Hollings P, Garven G, Brand U, Lécuyer C (2020) Evidence for Elevated and Variable Atmospheric Oxygen in the Precambrian. *Precambrian Research*, doi: 10.1016/j.precamres.2020.105722.

Sterne EJ, Zantop H, Reynolds RC (1984) Clay mineralogy and carbon-nitrogen geochemistry of the Lik and Competition Creek zinc-lead-silver prospects, DeLong Mountains, Alaska. *Economic Geology,* **79**, 1406-1411.

Stüeken EE, Kipp MA, Koehler MC, Buick R (2016) The evolution of Earth's biogeochemical nitrogen cycle. *Earth Science Reviews,* **160**, 220-239.

Stüeken EE, Zaloumis J, Meixnerová J, Buick R (2017) Differential metamorphic effects on nitrogen isotopes in kerogen extracts and bulk rocks. *Geochimica et Cosmochimica Acta,* **217**, 80-94.

Taylor MI, McMillan NE, Dalrymple IJ, Hayward N (2017) Teena zinc-lead deposit. In: *AusIMM Monograph 32 (Australian Ore Deposits)* (ed Phillips GN)*,* pp. 483-484.

Taylor RD, Leach DL, Bradley DC, Pisarevsky SA (2009) Compilation of mineral resource data for Mississippi Valley-type and clastic-dominated sediment-hosted lead-zinc deposits. *U.S. Geological Survey Open-File Report 2009-1297*, 1-42.

Williams N (1978) Studies of the base metal sulfide deposits at McArthur River, Northern Territory, Australia; II, The sulfide-S and organic-C relationships of the concordant deposits and their significance. *Economic Geology,* **73**, 1036-1056.

Williford KH, Grice K, Logan GA, Chen J, Huston D (2011) The molecular and isotopic effects of hydrothermal alteration of organic matter in the Paleoproterozoic McArthur River Pb/Zn/Ag ore deposit. *Earth and Planetary Science Letters,* **301**, 382-392.

Yoshiya K, Sawaki Y, Nishizawa M, Komiya T, Hirata T, Maruyama S (2015) In-situ iron isotope analysis of pyrite and organic carbon/nitrogen isotope ratios from teh Middle Proterozoic sediments. In: *Japan Geoscience Union Meeting*. Japan Geoscience Union, Makuhari, Chiba, Japan*,* pp. BPT23-15.